Semiclassical initial value representation for rotational degrees of freedom: The tunneling dynamics of HCl dimer

Xiong Sun and William H. Miller
Department of Chemistry, University of California, Berkeley, California and Chemical Sciences Division, Lawrence Berkeley Laboratory, Berkeley, California 94720

(Received 23 December 1997; accepted 24 February 1998)

The semiclassical initial value representation (SC-IVR) is emerging as a practical way of generalizing classical trajectory simulation methods to include (approximately) the effects of quantum mechanics (i.e., interference and tunneling). This paper describes the application of the SC-IVR approach to determine the low lying vibrational states of the HCl dimer on a realistic potential energy surface. Overall agreement of the semiclassical energy levels with accurate quantum values is very good, including a good description of the tunneling splitting in the ground state. Issues regarding the applications of the SC-IVR methodology to the angular variables related to rotational degrees of freedom are explicitly discussed. © *1998 American Institute of Physics.* [S0021-9606(98)01121-0]

I. INTRODUCTION

Semiclassical (SC) methods have a long history in chemical physics,[1–8] the attraction being that they provide a way, in principle, of augmenting classical trajectory simulation methods with an approximate inclusion of quantum mechanical effects. Many applications of SC theory in the early 1970's showed that, in effect, *all* quantum mechanical effects—interference (or coherence) effects, tunneling (including ''dynamic tunneling''), symmetry-based selection rules, scattering resonances (i.e., ''weak quantization'' of metastable states), and energy quantization of bound molecular systems—are contained in the SC description at least qualitatively, and that often the description is sufficiently accurate to be quite useful. A great deal was learned in this early work about the nature of quantum effects in molecular dynamics, but unfortunately the way that classical mechanics must be used in semiclassical theory makes it considerably more difficult to apply than ordinary classical mechanics. Thus the complexity (i.e., size) of the molecular system for which these semiclassical calculations could be carried out was considerably less than that for which ordinary classical trajectory simulations are practical.

Recently, however, there has been a revival of interest in using semiclassical methods for molecular dynamics simulations, based primarily on the *initial value representation* (IVR).[9–17] The IVR converts the multivalued *boundary value* problem of the conventional semiclassical approach into a single-valued *initial value* problem which is much easier to implement computationally; it also has an approximate ''uniformizing'' character that makes it typically more accurate than the original ''primitive'' semiclassical approximations. Though the IVR idea also originated in the early 1970's, recent work has introduced a variety of new IVR's that are more useful than the original version. The IVR version of SC theory has all the hallmarks noted above, i.e., inclusion of interference and tunneling effects, and a number of recent applications have illustrated its accuracy and usefulness for a variety of dynamical phenomena. Particularly interesting has been the generalization of the SC-IVR methodology to include *electronically nonadiabatic* processes,[18,19] i.e., dynamics involving transitions between different Born–Oppenheimer potential energy surfaces. By providing a unified treatment of the electronic and nuclear degrees of freedom, one avoids inconsistencies that arise in mixed quantum-classical approaches.

This paper describes the application of current SC-IVR methodology to the low lying eigenvalues of a van der Waals complex, namely the HCl dimer, thus further widening the class of dynamical problems for which the approach has been demonstrated. This is a truly benchmark van der Waals system, having been thoroughly studied experimentally by far-infrared spectroscopic techniques and a highly accurate potential energy surface developed to fit these data.[20] This is quite a nontrivial test for semiclassical theory because the strong hydrogen bonding in the system leads to strong anharmonic coupling between the rotational and vibrational degrees of freedom. The dissociation energy is only about 690 cm^{-1}, and there are two equivalent minima separated by a barrier of about 70 cm^{-1}. The low lying eigenvalues are thus characterized by tunneling splittings ($\sim$16 cm^{-1} for the lowest doublet) and other nonclassical effects. The goal of the present work is thus to see how well the SC-IVR approach is able to describe these phenomena.

Section II first briefly summarizes the SC-IVR approach and the Filinov, or stationary Monte Carlo smoothing methods used to implement it. The Appendix describes some special features of semiclassical mechanics that arise when treating angular coordinates for rotational degrees of freedom, and especially how the SC-IVR simplifies these matters. Specifics of the HCl dimer, i.e., the Hamiltonian, are discussed in Sec. III, and the results in Sec. IV. Section V concludes with some thoughts as to where one is in the SC-IVR program.

II. THE SEMICLASSICAL INITIAL VALUE REPRESENTATION

The basic idea of the SC-IVR is very simple. Consider, for example, the transition amplitude from state 1 to state 2 (i.e., a generic matrix element of the time evolution operator),

$$S_{2,1} \equiv \langle \Psi_2 | e^{-i\hat{H}t/\hbar} | \Psi_1 \rangle = \int d\mathbf{q}_2 \int d\mathbf{q}_1 \Psi(\mathbf{q}_2)^* \langle \mathbf{q}_2 | e^{-i\hat{H}t/\hbar} | \mathbf{q}_1 \rangle \Psi_1(\mathbf{q}_1). \tag{2.1}$$

Replacing the coordinate matrix representation of the propagator with the standard semiclassical (Van Vleck) approximation yields

$$S_{2,1} = \int d\mathbf{q}_2 \int d\mathbf{q}_1 \Psi_2(\mathbf{q}_2)^* \Psi_1(\mathbf{q}_1) \times \sum_{\text{roots}} \left[(2\pi i\hbar)^F \left| \frac{\partial \mathbf{q}_2}{\partial \mathbf{p}_1} \right| \right]^{-\frac{1}{2}} e^{iS_t(\mathbf{q}_2,\mathbf{q}_1)/\hbar - i\nu\pi/2}, \tag{2.2}$$

where

$$S_t(\mathbf{q}_2,\mathbf{q}_1) = \int_0^t d\tau [\mathbf{p}(\tau)\cdot\dot{\mathbf{q}}(\tau) - H(\mathbf{p}(\tau),\mathbf{q}(\tau))], \tag{2.3}$$

is the classical action for the trajectory that goes from $\mathbf{q}_1$ to $\mathbf{q}_2$ in time t. To apply Eq. (2.2) as written, one needs to solve a nonlinear boundary value problem; i.e., if $\mathbf{q}_t(\mathbf{p}_1,\mathbf{q}_1)$ is the coordinate at time t that evolves from the initial $(t=0)$ conditions $(\mathbf{p}_1,\mathbf{q}_1)$, then for a given $\mathbf{q}_t$, one must find values of $\mathbf{p}_1$ that satisfy

$$\mathbf{q}_t(\mathbf{p}_1,\mathbf{q}_1) = \mathbf{q}_2. \tag{2.4}$$

In general, there will be multiple roots to this equation (since $\mathbf{q}_t$ need not be a monotonic function of $\mathbf{p}_1$), and the summation in Eq. (2.2) is over all such roots. The Jacobian factor in Eq. (2.2),

$$\left| \frac{\partial \mathbf{q}_2}{\partial \mathbf{p}_1} \right| = \left| \frac{\partial \mathbf{q}_t(\mathbf{p}_1,\mathbf{q}_1)}{\partial \mathbf{p}_1} \right|, \tag{2.5}$$

is evaluated at the roots of Eq. (2.4), and ν is the number of zeros experienced by the determinant $|\partial \mathbf{q}_t/\partial \mathbf{p}_1|$ in the time interval $(0,t)$.

The idea of the initial value representation is to change the integral over the final coordinates in Eq. (2.2) to one over the initial momenta, giving

$$S_{2,1} = \int d\mathbf{p}_1 \int d\mathbf{q}_1 \Psi_2(\mathbf{q}_t)^* \Psi_1(\mathbf{q}_1) \times \left[\frac{|\partial \mathbf{q}_t/\partial \mathbf{p}_1|}{(2\pi i\hbar)^F} \right]^{1/2} e^{iS_t(\mathbf{p}_1,\mathbf{q}_1)/\hbar - i\pi\nu/2}, \tag{2.6}$$

where $S_t(\mathbf{p}_1,\mathbf{q}_1) = S(\mathbf{q}_t(\mathbf{p}_1,\mathbf{q}_1),\mathbf{q}_1)$. Equation (2.6), though formally identical to Eq. (2.2), has several advantages over it, the most important is that the classical trajectories needed to evaluate the integral are specified by their *initial* conditions $(\mathbf{p}_1,\mathbf{q}_1)$ and not by the double-ended *boundary* conditions $(\mathbf{q}_2,\mathbf{q}_1)$. This also means that the summation in Eq. (2.2) is no longer present because initial conditions determine a unique classical trajectory. Stated more precisely, for a given $\mathbf{q}_1$,

$$\int d\mathbf{q}_2 \sum_{\text{roots}} \rightarrow \int d\mathbf{p}_1 \left| \frac{\partial \mathbf{q}_t}{\partial \mathbf{p}_1} \right|. \tag{2.7}$$

Another benefit of the IVR is that the Jacobian from the change of integration variables in Eq. (2.7) combines with the denominator in Eq. (2.2), so that the square root of the Jacobian now appears in the numerator of Eq. (2.6). Since this factor can go through zero, having it in the numerator removes singularities in the integrand and thus facilitates numerical integration. Additionally, this Jacobian factor causes the integrand to be zero when ν changes discontinuously, so that the integrand is continuous at these points.

An IVR, however, is not unique. Equation (2.6) is obtained by beginning with the propagator in a coordinate representation, but another result is obtained if one begins with a momentum representation. Herman and Kluk[11] made a very useful contribution in showing how to combine these two possibilities by using a coherent state representation (motivated by the ''frozen Gaussian'' approximation of Heller[21]); the Herman–Kluk (HK) IVR is

$$\langle \Psi_2 | e^{-i\hat{H}t/\hbar} | \Psi_1 \rangle = \int \frac{d\mathbf{p}_1 d\mathbf{q}_1}{(2\pi\hbar)^F} C_t(\mathbf{p}_1,\mathbf{q}_1) \times e^{iS_t(\mathbf{p}_1,\mathbf{q}_1)/\hbar} \langle \Psi_2 | \mathbf{p}_t,\mathbf{q}_t \rangle \times \langle \mathbf{p}_1,\mathbf{q}_1 | \Psi_1 \rangle, \tag{2.8}$$

where $\langle \mathbf{p},\mathbf{q}|\Psi\rangle$ is the coherent state representation of the wave function $|\Psi\rangle$,

$$\langle \mathbf{p},\mathbf{q}|\Psi\rangle = \int d\mathbf{x} \left(\frac{\gamma}{\pi} \right)^{F/4} e^{-\gamma/2(\mathbf{x}-\mathbf{q})^2 - i/\hbar \mathbf{p}\cdot(\mathbf{x}-\mathbf{q})} \Psi(\mathbf{x}), \tag{2.9}$$

and

$$C_t(\mathbf{p}_1,\mathbf{q}_1) = \left| \tfrac{1}{2} \left(\frac{\partial \mathbf{q}_t}{\partial \mathbf{q}_1} + \frac{\partial \mathbf{p}_t}{\partial \mathbf{p}_1} - i\gamma\hbar \frac{\partial \mathbf{q}_t}{\partial \mathbf{p}_1} + \frac{i}{\gamma\hbar} \frac{\partial \mathbf{p}_t}{\partial \mathbf{q}_1} \right) \right|^{\frac{1}{2}}. \tag{2.10}$$

It is not hard to show that in the limit of $\gamma \rightarrow \infty$, Eq. (2.8) reduces to the coordinate space IVR of Eq. (2.6), while the limit $\gamma \rightarrow 0$ gives the momentum space IVR. Kay has made a rather extensive study of this by treating a variety of these IVR's,[10] concluding that the HK version often seems to be most accurate overall. This has also been our experience and is thus used in the present application.

The computational task in a SC-IVR calculation is therefore a phase space average over the initial conditions of classical trajectories, the chief difficulty of which is caused by the fact that the integrand is oscillatory. Furthermore, the preexponential factor in the integrand—the factor $C_t(\mathbf{p},\mathbf{q})$ in Eq. (2.8)—tends to increase roughly algebraically with t if the trajectory is regular and exponentially if it is chaotic, so the amplitude of the oscillation grows with time. Applications to date have dealt with this problem by using ''filter-

ing'' or stationary phase Monte Carlo methods[22,23] to damp the oscillations of the integrand. Consider, for example, a generic oscillatory integral of the form

$$I=\int d\mathbf{x} g(\mathbf{x}) e^{if(\mathbf{x})}. \tag{2.11}$$

The Filinov[22] smoothing approach replaces this by

$$I=\int d\mathbf{x}\left|\mathbf{1}-\frac{i}{c}\frac{\partial^2 f}{\partial\mathbf{x}\partial\mathbf{x}}\right|^{-1/2} g(\mathbf{x}) \times\exp\left[if(\mathbf{x})-\frac{1}{2c}\frac{\partial f}{\partial\mathbf{x}}\cdot\left(\mathbf{1}-\frac{i}{c}\frac{\partial^2 f}{\partial\mathbf{x}\partial\mathbf{x}}\right)^{-1}\cdot\frac{\partial f}{\partial\mathbf{x}}\right]. \tag{2.12}$$

This smoothing procedure can be applied to any of the IVR's discussed here, and there is also some flexibility with the choice of the functions f and g. After some investigation, we conclude that the Filinov transformation applied to the HK IVR, as suggested by Walton and Manolopoulos,[14a] is the most effective one so far. All the SC-IVR calculations reported in this paper are performed with this approach.

To determine the eigenvalues of a bound molecular system, which is the application of interest in this paper, we consider the spectral density with respect to some reference wave function $|\Psi\rangle$,

$$J(E)=\langle\Psi|\delta(E-\hat{H})|\Psi\rangle, \tag{2.13}$$

which of course has delta function peaks at the the eigenvalues $\{E_k\}$ of the Hamiltonian,

$$J(E)=\sum_k |\langle\Psi|\Psi_k\rangle|^2\delta(E-E_k), \tag{2.14}$$

where $|\Psi_k\rangle$ are the corresponding eigenfunctions. The microcanonical density operator $\delta(E-\hat{H})$ can be expressed in terms of the propagator in the usual way,

$$\delta(E-\hat{H})=-\frac{1}{\pi}\,\mathrm{Im}\,\hat{G}(E), \tag{2.15}$$

$$\hat{G}(E)=\frac{1}{i\hbar}\int_0^\infty e^{iEt/\hbar}e^{-i\hat{H}t/\hbar}, \tag{2.16}$$

so that the spectrum is given in terms of the propagator by

$$J(E)=\mathrm{Re}\,\frac{1}{\pi\hbar}\int_0^\infty e^{iEt/\hbar}\langle\Psi|e^{-i\hat{H}t/\hbar}|\Psi\rangle. \tag{2.17}$$

The semiclassical approximation corresponds to using an IVR of choice for the diagonal matrix element of the propagator in Eq. (2.17). In practice, one also typically includes a convergence factor to cut off the time integral in Eq. (2.17), e.g., a Gaussian, to obtain

$$J(E)=\mathrm{Re}\,\frac{1}{\pi\hbar}\int_0^\infty e^{iEt/\hbar-(1/2)\Delta E^2t^2/\hbar^2}\langle\Psi|e^{-i\hat{H}t/\hbar}|\Psi\rangle, \tag{2.18}$$

for which the corresponding quantum expression that replaces Eq. (2.14) is

$$J(E)=\sum_k |\langle\Psi|\Psi_k\rangle|^2\frac{e^{-(\frac{1}{2})(E-E_k)^2/\Delta E^2}}{\sqrt{2\pi}\Delta E}. \tag{2.19}$$

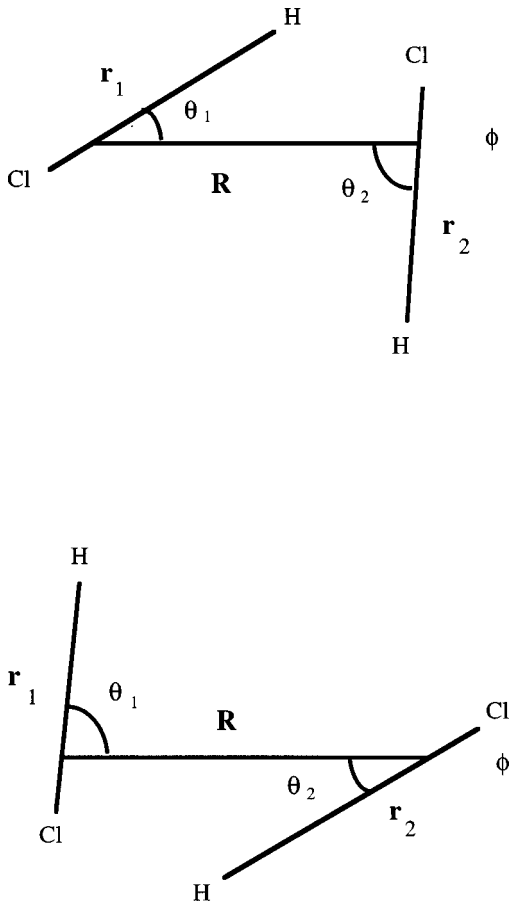

FIG. 1. The two equilibrium configurations of the HCl dimer. The values of the coordinates are $R=3.746$ Å, $\phi=180$, $\theta_1=9°$, $\theta_2=89.8°$. The HCl monomer bond lengths are fixed.

In practice, one chooses ΔE as large as possible—so as to make the time integral in Eq. (2.17) converge in as short a time as possible—but not so large that the Gaussian peaks in Eq. (2.19) overlap too much for the individual eigenvalues to be resolved. Lastly, it is worth noting that in one dimension, the semiclassical quantization condition derived from Eq. (2.17) (with a stationary phase evaluation of the time integral) is identical to the Wentzel–Kramers–Brillouin (WKB) quantization. Thus, this method of finding the eigenvalue can be viewed as a multidimensional generalization of the WKB analysis.

III. THE HCl DIMER HAMILTONIAN

In terms of the standard Jacobi coordinates shown in Fig. 1—$\mathbf{r}_1$ and $\mathbf{r}_2$ for the two diatomic monomers, and $\mathbf{R}$ the center of mass coordinate between the two—and their conjugate momenta, the classical Hamiltonian for the diatom–diatom system is

$$H=\frac{P_R^2}{2\mu}+\frac{l^2}{2\mu R^2}+\frac{p_{r_1}^2}{2m_1}+\frac{j_1^2}{2m_1r_1^2}+\frac{p_{r_2}^2}{2m_2}+\frac{j_2^2}{2m_2r_2^2}+V, \tag{3.1}$$

where $\mathbf{j}_n=\mathbf{r}_n\times\mathbf{p}_n$, for $n=1$ and 2, and $\mathbf{l}=\mathbf{R}\times\mathbf{P}$. m_1, m_2, and μ are the appropriate reduced masses (and here, of course, $m_1=m_2=m$). Using the Van Vleck body-fixed axis

procedure,[24] we choose **R** as the body-fixed axis, and the angular momentum of this axis, **l**, is eliminated by the use of total angular momentum conservation,

$$\mathbf{l}=\mathbf{J}-(\mathbf{j}_1+\mathbf{j}_2), \tag{3.2}$$

where **J** is the total angular momentum. In the present application, we consider only zero total angular momentum, $J=0$, and also take the two monomer HCl's to be rigid rotors, thus setting the two radial momenta $p_{r_1}=p_{r_2}=0$. The Hamiltonian thus becomes

$$H=\frac{P_R}{2\mu}+\frac{|\mathbf{j}_1+\mathbf{j}_2|^2}{2\mu R^2}+B(j_1^2+j_2^2)+V, \tag{3.3}$$

where $B=(2mr^2)^{-1}$ is (with $\hbar=1$) the monomer HCl rotation constant ($B=10.44\ \mathrm{cm}^{-1}$). The rotational angular momenta of the two monomers, $\mathbf{j}_1$ and $\mathbf{j}_2$, are given by the standard expressions[25] in terms of the polar and azimuthal angles (θ_1,ϕ_1) and (θ_2,ϕ_2) that orient $\mathbf{r}_1$ and $\mathbf{r}_2$ with respect to the body-fixed axis **R**, and their conjugate momenta, as

$$\mathbf{j}_n=\begin{pmatrix} -p_{\theta_n}\sin\phi_n-\cos\phi_n\cot\theta_n p_{\phi_n} \\ p_{\theta_n}\cos\phi_n-\sin\phi_n\cot\theta_n p_{\phi_n} \\ p_{\phi_n}\end{pmatrix}, \tag{3.4}$$

for $n=1$ and 2. In Eq. (3.3), one thus has

$$j_n^2=p_{\theta_n}^2+\frac{p_{\phi_n}^2}{\sin^2\theta_n}, \tag{3.5}$$

$$\begin{aligned}\mathbf{j}_1\cdot\mathbf{j}_2=&\,p_{\theta_1}p_{\theta_2}\cos(\phi_1-\phi_2)\\&+p_{\phi_1}p_{\phi_2}[\cot\theta_1\cot\theta_2\cos(\phi_1-\phi_2)+1]\\&+p_{\theta_1}p_{\phi_2}\cot\theta_2\sin(\phi_1-\phi_2)\\&+p_{\theta_2}p_{\phi_1}\cot\theta_1\sin(\phi_2-\phi_1).\end{aligned} \tag{3.6}$$

Finally, since the Hamiltonian (including the potential V) depends only on the difference of the two azimuthal angles $\phi_1-\phi_2$, and not their sum, one makes a canonical transformation to the sum and difference variables,

$$\begin{aligned}&\phi=\phi_1-\phi_2,\quad \Phi=\tfrac{1}{2}(\phi_1+\phi_2),\\&p_\phi=\tfrac{1}{2}(p_{\phi_1}-p_{\phi_2}),\quad p_\Phi=p_{\phi_1}+p_{\phi_2}.\end{aligned} \tag{3.7}$$

The Hamiltonian, as noted before, is independent of Φ, so that p_Φ is conserved (and equal to 0 for $J=0$). Putting all this together, the final form for the $J=0$ Hamiltonian involves four degrees of freedom, $(R,\theta_1,\theta_2,\phi)$ and their conjugate momenta, and is given explicitly by

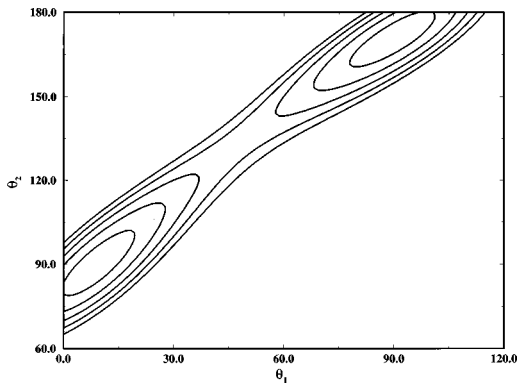

FIG. 2. Contours of potential energy surface of the HCl dimer in the θ_1 and θ_2 plane from -690 to $-550\ \mathrm{cm}^{-1}$. The other coordinates are held at their equilibrium values.

$$\begin{aligned}&H(P_R,R,p_{\theta_1},\theta_1,p_{\theta_2},\theta_2,p_\phi,\phi)\\&=\frac{P_R^2}{2\mu}+\left(B+\frac{1}{2\mu R^2}\right)\left(p_{\theta_1}^2+\frac{p_\phi^2}{\sin^2\theta_1}+p_{\theta_2}^2+\frac{p_\phi^2}{\sin^2\theta_2}\right)\\&\quad\times\frac{1}{\mu R^2}[p_{\theta_1}p_{\theta_2}\cos\phi-p_\phi^2(\cot\theta_1\cot\theta_2\cos\phi+1)\\&\quad-p_\phi\sin\phi(p_{\theta_1}\cot\theta_2+p_{\theta_2}\cot\theta_1)]\\&\quad+V(R,\theta_1,\theta_2,\phi).\end{aligned} \tag{3.8}$$

The potential energy surface V has been determined by Elrod *et al.*[20] in the form of the following expansion,

$$V(R,\theta_1,\theta_2,\phi)=\sum_{l_1l_2l}A_{l_1l_2l}(R)g_{l_1l_2l}(\theta_1,\theta_2,\phi), \tag{3.9}$$

the parameters for which are determined by fitting quantum mechanical calculations to the experimental spectra. Figure 2 shows a contour plot of the potential surface as a function of (θ_1,θ_2) for planar geometry ($\phi=180°$) and a fixed value of R. This clearly displays the $\theta_1\leftrightarrow\theta_2$ exchange symmetry and the two equivalent minima indicated in Fig. 1. As noted in the Introduction, the barrier separating the two minima ($\sim 70\ \mathrm{cm}^{-1}$) is sufficiently low that tunneling between them gives rise to a splitting of about $16\ \mathrm{cm}^{-1}$ between the lowest two energy levels. Even and odd states with respect to this $\theta_1\leftrightarrow\theta_2$ exchange are designated by A and B, respectively. The potential is also symmetric in the out-of-plane coordinate ϕ, so that the states are also even or odd with respect to $\phi\rightarrow 2\pi-\phi$. This symmetry is designated + or −. The states thus have four possible symmetries in this system, A^+,A^-,B^+,B^-.

IV. RESULTS AND DISCUSSION

The reference wave function in Eq. (2.17) is, to some extent, arbitrary, the primary requirement being that it has significant overlap with the states whose energy levels one is wishing to extract from the calculation. One may in fact wish to use several different reference wave functions. Because the Herman–Kluk IVR expression [Eq. (2.8)] involves coherent states, it is natural to choose Ψ also of this form. Thus, we have used a direct product of such functions,

$$\Psi(R,\theta_1,\theta_2,\phi)=\psi_1(R)\psi_2(\theta_1)\psi_3(\theta_2)\psi_4(\phi), \tag{4.1}$$

where each factor is related to a coherent state,

$$\psi_1(R)=\left(\frac{\gamma_1}{\pi}\right)^{1/4} R^{-2} e^{-(\gamma_1/2)(R-R_0)^2+iP_{R0}(R-R_0)/\hbar}, \tag{4.2}$$

$$\psi_2(\theta_1)=\left(\frac{\gamma_2}{\pi}\right)^{1/4} (\sin\,\theta_1)^{-1} e^{-(\gamma_2/2)(\theta_1-\theta_{10})^2+iP_{\theta_1 0}(\theta_1-\theta_{10})/\hbar}, \tag{4.3}$$

$$\psi_3(\theta_2)=\left(\frac{\gamma_3}{\pi}\right)^{1/4} (\sin\,\theta_2)^{-1} e^{-(\gamma_3/2)(\theta_2-\theta_{20})^2+iP_{\theta_2 0}(\theta_2-\theta_{20})/\hbar}, \tag{4.4}$$

$$\psi_4(\phi)=\left(\frac{\gamma_4}{\pi}\right)^{1/4} e^{-(\gamma_4/2)(\phi-\phi_0)^2+iP_{\phi 0}(\phi-\phi_0)/\hbar}, \tag{4.5}$$

where R^{-2} and $(\sin\,\theta_n)^{-1}$ will cancel with the Jacobian factors when calculating the overlap $\langle \mathbf{q},\mathbf{p}|\Psi\rangle$, and the coherent state widths $\{\gamma_i\}$ are chosen large enough so that the following approximation,

$$\begin{aligned}\langle \mathbf{q},\mathbf{p}|\Psi\rangle &= \int_0^\infty dR \int_0^\pi d\theta_1 \int_0^\pi d\theta_2 \int_0^{2\pi} d\phi\; R^2 \\ &\quad \times \sin\,\theta_1\, \sin\,\theta_2 \Psi(R,\theta_1,\theta_2,\phi) \\ &\quad \times \langle \mathbf{q},\mathbf{p}|R,\theta_1,\theta_2,\phi\rangle \\ &\approx \int_{-\infty}^\infty dR \int_{-\infty}^\infty d\theta_1 \int_{-\infty}^\infty d\theta_2 \int_{-\infty}^\infty d\phi\; R^2 \\ &\quad \times \sin\,\theta_1\, \sin\,\theta_2 \Psi(R,\theta_1,\theta_2,\phi) \\ &\quad \times \langle \mathbf{q},\mathbf{p}|R,\theta_1,\theta_2,\phi\rangle,\end{aligned} \tag{4.6}$$

is valid. Actually, we use a linear combination of functions of the type in Eq. (4.1) in order to take advantage of symmetry: to determine the energy levels for a given symmetry, one chooses the reference wave function to be of this symmetry so that only states with this symmetry will appear in the spectral density [as most easily seen in the quantum expression, Eq. (2.14)]. In the present case, for example, the reference wave function of Eq. (4.1) is modified as follows,

$$\begin{aligned}\Psi_{\sigma,\sigma'}(R,\theta_1,\theta_2,\phi) &= \psi_1(R)[\psi_2(\theta_1)\psi_3(\theta_2) \\ &\quad + \sigma\psi_2(\theta_2)\psi_3(\theta_1)] \\ &\quad \times [\psi_4(\phi)+\sigma'\psi_4(2\pi-\phi)],\end{aligned} \tag{4.7}$$

where $\sigma\sigma'=++$, $+-$, $-+$, and $--$ correspond to the A^+, A^-, B^+, and B^- states, respectively. The semiclassical calculation can thus be carried out separately for each symmetry.

Figure 3 shows a typical semiclassical correlation function $\langle \Psi|e^{-i\hat{H}t/\hbar}|\Psi\rangle$ for A^+ symmetry. It is obtained with $\sim$3000 bounded classical trajectories whose initial conditions are chosen by Monte Carlo from the coherent state overlap with the reference wave function, $|\langle \mathbf{q},\mathbf{p}|\Psi\rangle|$. (Trajectories which dissociated are discarded since their Fourier transform cannot contribute to delta function peaks in the energy spectrum.) Figures 4 and 5 show the energy spectra obtained from the SC-IVR correlation functions, indicating the peaks corresponding to the energy levels. No attempt was made at using more sophisticated ''signal processing'' algorithms[26] to extract the energy levels from the time correlation function, though this would perhaps make the overall procedure more efficient.

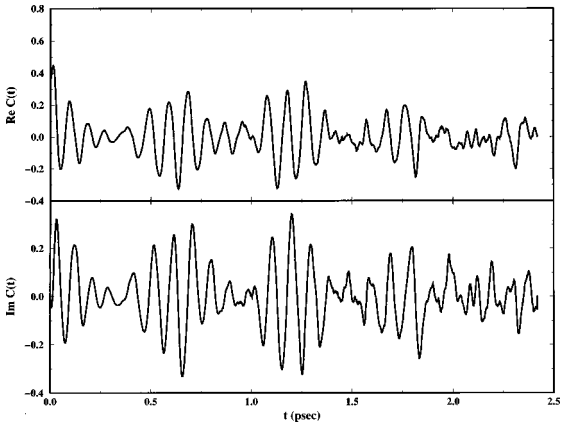

FIG. 3. The real and imaginary parts of the semiclassical correlation function, $\langle \Psi|e^{-i\hat{H}t/\hbar}|\Psi\rangle$, where Ψ is of A^+ symmetry. This is obtained with about 3000 bound trajectories.

The lowest few SC-IVR energy levels of each symmetry are listed in Table I, along with the corresponding quantum mechanical (QM) values calculated by Elrod *et al.*[20] The SC-IVR and QM energy levels are listed relative to the ground state of each, and one sees quite good agreement overall. The average error in the semiclassical energy levels for these states is 1.65 cm^{-1}, with the maximum being about 4 cm^{-1}. It is particularly interesting to see that the tunneling splitting of the ground state—the difference of the lowest A^+ and B^+

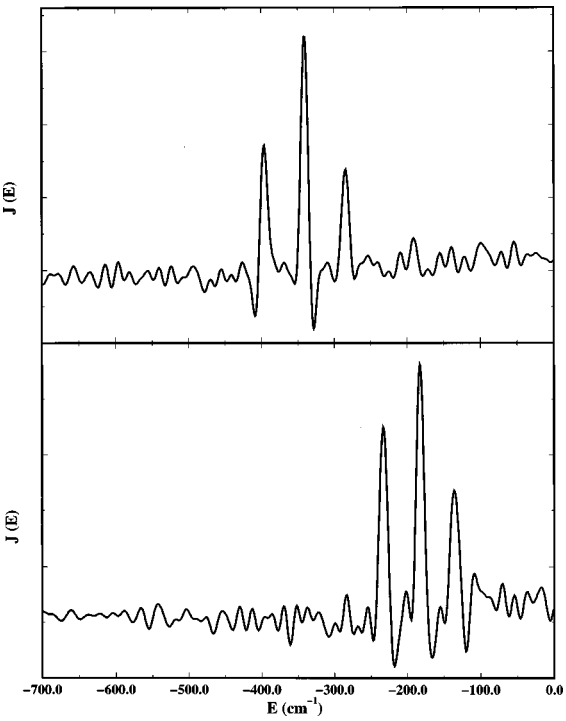

FIG. 4. Representative spectra for A^+ (upper panel) and A^- (lower panel) symmetries.

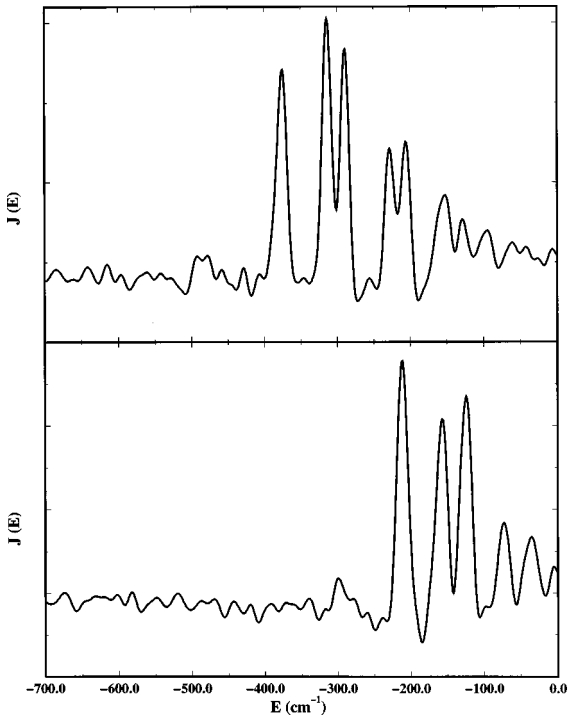

FIG. 5. Representative spectra for B^+ (upper panel) and B^- (lower panel) symmetries.

energy levels—is described reasonably well, 18 cm^{-1} compared to the correct value of 15.7 cm^{-1}. We consider this level of success for the SC-IVR model to be excellent and further evidence that it is capable of describing a wide range of dynamical phenomena to a useful accuracy, even at the most detailed level where quantum effects are very significant.

The result obtained for the SC-IVR ground state (-395.5 cm^{-1}), however, is 16.3 cm^{-1} above the quantum ground state (-411.8 cm^{-1}). Therefore, on an absolute energy scale, all SC-IVR energy levels are about this much larger than the corresponding QM values. From the discussion at the end of the Appendix, it is not surprising that the SC energies are shifted by an approximately constant value relative to the QM ones, but it is not easy to reconcile the value of the shift (16.3 cm^{-1}) we observe. If the two HCl rigid diatomics were free rotors, then the discussion in the Appendix shows that the SC energy levels would be $\frac{1}{2}B$ above the QM values ($\frac{1}{4}B$ for each rotor), and since the rotation constant of HCl is $B=10.44$ cm^{-1}, this suggests a shift of about 5.2 cm^{-1}. (We in fact carried out the SC-IVR calculation for the uncoupled case and did indeed obtain energy levels shifted by this amount.) Why one obtains a significantly larger shift than this for the fully coupled case is not clear to us, but it is nevertheless reassuring that the SC-IVR energy levels are good approximations to the QM values for *some* constant (and modest) shift.

TABLE I. Comparison of semiclassical and quantum mechanical energy levels (in cm^{-1}) for $(HCl)_2$, for $J=0$ and various molecular symmetries.

	QM	SC-IVR
A^+	0.0[a]	0.0[a]
	53.3	55.5
	72.1	76.6
	111.2	111.4
	147.8	147.8
A^-	160.6	162.6
	212.0	212.7
B^+	15.7	18.0
	79.6	80.9
	104.0	106.7
	167.5	166.4
	188.0	190.8
B^-	185.1	186.7
	240.3	240.0

[a]QM and SC-IVR energy levels are shown relative to the ground state of each. The SC-IVR ground state is 16.3 cm^{-1} above the QM ground state.

V. CONCLUDING REMARKS

In summary, we have presented an application of the semiclassical (SC) initial value representation (IVR) to a highly nontrivial multidimensional system, involving dynamics on a very anharmonic potential energy surface with multiple wells. We obtain the ground and excited state vibrational energy levels of each symmetry to a good level of accuracy with a relatively modest number of classical trajectories. Perhaps the most important dynamical quantity, the tunneling splitting of the ground state, is obtained to good accuracy. These results help to further make the case that the SC-IVR model provides a unified dynamical approach for molecular dynamics simulations that includes essentially all quantum effects to a very good approximation.

For the SC-IVR approach to be a *practical* TOE (''theory of everything'') for chemical physics, however, one must be able to carry out the calculation for more complex (i.e., larger) molecular systems. It is possible, of course, to carry out classical trajectory calculations for systems with hundreds (or more) of atoms and molecules, and the goal is to be able to implement the SC-IVR methodology for such systems. As noted, the trajectories can be calculated, but it is the phase space average over the initial conditions of an oscillatory integrand [cf. Eq. (2.8)] that is the computational bottleneck. The various filtering methods noted in Sec. II have made it possible to do the various calculations reported to date, but one needs to make additional progress in order to break out of the small molecule dynamics arena. There are several new avenues that have been suggested for dealing with this but their usefulness is yet to be demonstrated. The potential payoff is so great that this problem warrants considerable research effort.

ACKNOWLEDGMENTS

The authors would like to thank Linda Braly and Richard Saykally for providing the $(HCl)_2$ potential energy surface. This work has been supported by the Director, Office of Energy Research, Office of Basic Energy Sciences, Chemical Sciences Division of the U.S. Department of Energy under Contract No. DE-AC03-76SF00098, and also in part by the National Science Foundation under Grant No. CHE9422559.

APPENDIX: SPECIAL CONSIDERATIONS OF THE SC-IVR FOR ANGULAR COORDINATES

Here we note some specific features of the SC-IVR when treating angular variables for rotational degrees of freedom. Consider first a one dimensional rotor whose orientation in a plane is characterized by angle ϕ, with the Hamiltonian

$$\hat{H}=-\frac{\hbar^2}{2I}\frac{d^2}{d\phi^2}+V(\phi), \tag{A1}$$

where I is the moment of inertia. A typical matrix element of the propagator thus has the form

$$S_{2,1}\equiv\langle\Psi_2|e^{-i\hat{H}t/\hbar}|\Psi_1\rangle = \int_0^{2\pi}d\phi_1\int_0^{2\pi}d\phi_2\Psi_2(\phi_2)^*\langle\phi_2|e^{-i\hat{H}t/\hbar}|\phi_1\rangle\Psi_1(\phi_1), \tag{A2}$$

with the wave functions normalized on the interval $(0,2\pi)$ in the usual way,

$$\int_0^{2\pi}d\phi|\Psi(\phi)|^2=1. \tag{A3}$$

If $K_t(\phi_2,\phi_1)$ is the standard semiclassical amplitude for the $\phi_1\rightarrow\phi_2$ transition in time t, i.e.,

$$K_t(\phi_2,\phi_1)=\sum\left[2\pi i\hbar\left|\frac{\partial\phi_t}{\partial p_{\phi_1}}\right|\right]^{-1/2}e^{iS_t(\phi_2,\phi_1)/\hbar}, \tag{A4}$$

then the new feature that arises here is that the net amplitude for the transition must take account of the fact that all final angles $\phi_2+2\pi n$ ($n=$ any integer) correspond to the same physical orientation as angle ϕ_2, so that the amplitude in the integrand of Eq. (A2) must be a sum over all these symmetrically equivalent final angles,

$$\langle\phi_2|e^{-i\hat{H}t/\hbar}|\phi_1\rangle=\sum_{n=-\infty}^{\infty}K_t(\phi_2+2\pi n,\phi_1). \tag{A5}$$

Equation (A2) thus reads

$$S_{2,1}=\sum_{n=-\infty}^{\infty}\int_0^{2\pi}d\phi_1\int_0^{2\pi}d\phi_2\Psi_2(\phi_2)^*K_t(\phi_2+2\pi n,\phi_1)\times\Psi_1(\phi_1), \tag{A6}$$

and if one changes the integration variable from ϕ_2 to $\phi_2'=\phi+2\pi n$, it becomes

$$S_{2,1}=\sum_{n=-\infty}^{\infty}\int_0^{2\pi}d\phi_1\int_{2\pi n}^{2\pi(n+1)}d\phi_2' \times\Psi_2(\phi_2')^*K_t(\phi_2',\phi_1)\Psi_1(\phi_1), \tag{A7}$$

where it has been assumed that the wave function Ψ_2 is periodic, i.e., $\Psi_2(\phi_2'-2\pi n)=\Psi_2(\phi_2')$. But,

$$\sum_{n=-\infty}^{\infty}\int_{2\pi n}^{2\pi(n+1)}d\phi_2'=\int_{-\infty}^{\infty}d\phi_2', \tag{A8}$$

so that Eq. (A7) becomes

$$S_{2,1}=\int_0^{2\pi}d\phi_1\int_{-\infty}^{\infty}d\phi_2\Psi_2(\phi_2)^*K_t(\phi_2,\phi_1)\Psi_1(\phi_1), \tag{A9}$$

where the prime has now been dropped from the integration variable ϕ_2'. The integral over the entire interval $(-\infty,\infty)$ of the final angle ϕ_2, together with the periodicity of the final wave function $\Psi_2(\phi_2)$, thus properly takes account of the sum over all symmetrically equivalent final angles in Eq. (A5). One now applies the standard IVR transformation to Eq. (A9), i.e.,

$$\int_{-\infty}^{\infty}d\phi_2=\int_{-\infty}^{\infty}dp_{\phi_1}\left|\frac{\partial\phi_t}{\partial p_{\phi_1}}\right|, \tag{A10}$$

to give the final result

$$\langle\Psi_2|e^{-i\hat{H}t/\hbar}|\Psi_1\rangle = \int_0^{2\pi}d\phi_1\int_{-\infty}^{\infty}dp_{\phi_1}\Psi_2(\phi_t)^*\left[\left|\frac{\partial\phi_t}{\partial p_{\phi_1}}\right|\Big/\,2\pi i\hbar\right]^{1/2} \times e^{iS_t(\phi_1,p_{\phi_1})/\hbar}\Psi_1(\phi_1), \tag{A11}$$

which is of the standard IVR form. With the wave function normalized in the standard way, the integral over the initial angle is thus over the primary interval $(0,2\pi)$ and that of the conjugate initial momentum is over all values $(-\infty,\infty)$.

To illustrate the importance of including all symmetrically equivalent final angles, consider the *free* plane rotor, i.e., $V(\phi)=0$ in Eq. (A1). The SC propagator of Eq. (A4) is then of the standard free particle form

$$K_t(\phi_2,\phi_1)=\sqrt{\frac{I}{2\pi i\hbar t}}\,e^{iI(\phi_2-\phi_1)^2/2\hbar t}, \tag{A12}$$

which give the following microcanonical density matrix,

$$\langle\phi_2|\delta(E-\hat{H})|\phi_1\rangle\equiv\frac{\mathrm{Re}}{\pi\hbar}\int_0^{\infty}dt e^{iEt/\hbar}K_t(\phi_2,\phi_1) = \frac{I}{\pi\hbar^2k}\cos[k(\phi_2-\phi_1)], \tag{A13}$$

where $k=\sqrt{2IE}/\hbar$. Including the sum over all equivalent final angles, however, changes this to

$$\langle\phi_2|\delta(E-\hat{H})|\phi_1\rangle = \frac{I}{\pi\hbar^2k}\sum_{n=-\infty}^{\infty}\cos[k(\phi_2-\phi_1)+2\pi nk], = \frac{I}{\pi\hbar^2k}\cos[k(\phi_2-\phi_1)]\sum_{n=-\infty}^{\infty}\cos(2\pi nk), \tag{A14}$$

and the Poisson sum formula,[27]

$$\sum_{n=-\infty}^{\infty}\cos(2\pi nk)=\sum_{l=-\infty}^{\infty}\delta(l-k), \tag{A15}$$

requires k to be an *integer*. This is therefore what quantizes the energy $E=\hbar^2k^2/2I$ and gives delta function peaks at these values in the matrix element of $\delta(E-\hat{H})$.

Finally, there is another feature in the semiclassical description of rotational motion that should be noted. Consider a free linear rotor in 3D space, for which the classical Hamiltonian is

$$H=\frac{1}{2I}\left(p_\theta^2+\frac{p_\phi^2}{\sin^2\theta}\right). \tag{A16}$$

Quantization of the ϕ motion, as discussed above, requires $p_\phi=m\hbar$, m an integer. The θ motion thus takes place in the centrifugal potential well $V(\theta)$,

$$V(\theta)=B\,\frac{m^2}{\sin^2\theta}, \tag{A17}$$

where $B=\hbar^2/2I$ is the rotational constant. The standard WKB (Bohr–Sommerfeld) quantization of this bound motion,

$$(n+\tfrac{1}{2})\pi=\int d\theta\sqrt{2I(E-V(\theta))}/\hbar, \tag{A18}$$

gives the following energy levels,

$$\begin{aligned} &E_{n,m}=B(n+\tfrac{1}{2}+|m|)^2,\\ &n=0,1,2,..., \end{aligned} \tag{A19}$$

or in terms of the usual quantum number $l=n+|m|$,

$$E_l=B(l+\tfrac{1}{2})^2=Bl(l+1)+\tfrac{1}{4}B. \tag{A20}$$

The semiclassical energy levels are thus too large by a constant value. In any applications to rotational problems, therefore, one may expect that energy level *spacings* given by the semiclassical theory will be more accurate than their absolute value.

[1] R. B. Bernstein, Adv. Chem. Phys. **10**, 75 (1966).
[2] M. V. Berry and K. E. Mount, Rep. Prog. Phys. **35**, 315 (1972).
[3] W. H. Miller, Adv. Chem. Phys. **25**, 69 (1974); **30**, 77 (1975); Science **233**, 171 (1986).
[4] I. C. Percival, Adv. Chem. Phys. **36**, 1 (1977).
[5] M. C. Gutzwiller, *Chaos in Classical and Quantum Mechanics* (Springer-Verlag, New York, 1990).
[6] D. W. Noid, M. L. Koszykowski, and R. A. Marcus, Annu. Rev. Phys. Chem. **32**, 267 (1981).
[7] E. J. Heller, Acc. Chem. Res. **14**, 368 (1981).
[8] M. S. Child, *Semiclassical Mechanics with Molecular Applications* (Oxford University Press, New York, 1991).
[9] W. H. Miller, J. Chem. Phys. **53**, 3578 (1970).
[10] K. G. Kay, J. Chem. Phys. **100**, 4377 (1994); **100**, 4432 (1994); **101**, 2250 (1994).
[11] M. F. Herman and E. Kluk, Chem. Phys. **91**, 27 (1984); E. Kluk, M. F. Herman, and H. L. Davis, J. Chem. Phys. **84**, 326 (1986).
[12] (a) D. Provost and P. Brumer, Phys. Rev. Lett. **74**, 250 (1995); (b) G. Campolieti and P. Brumer, Phys. Rev. A **50**, 997 (1994).
[13] (a) E. J. Heller, J. Chem. Phys. **94**, 2723 (1991); (b) W. H. Miller, *ibid.* **95**, 9428 (1991); (c) E. J. Heller, *ibid.* **95**, 9431 (1991).
[14] (a) A. R. Walton and D. E. Manolopoulos, Mol. Phys. **87**, 961 (1996); (b) A. R. Walton and D. E. Manolopoulos, Chem. Phys. Lett. **244**, 448 (1995).
[15] (a) S. Keshavamurthy and W. H. Miller, Chem. Phys. Lett. **218**, 189 (1994); (b) B. W. Spath and W. H. Miller, *ibid.* **262**, 486 (1996); (c) X. Sun and W. H. Miller, J. Chem. Phys. **106**, 916 (1997).
[16] K. G. Kay, J. Chem. Phys. **107**, 2313 (1997).
[17] (a) S. Garashchuk and D. J. Tannor, Chem. Phys. Lett. **262**, 477 (1996); (b) F. Grossmann, *ibid.* **262**, 470 (1996).
[18] X. Sun and W. H. Miller, J. Chem. Phys. **106**, 6346 (1997).
[19] G. Stock and M. Thoss, Phys. Rev. Lett. **78**, 578 (1997).
[20] M. J. Elrod and R. J. Saykally, J. Chem. Phys. **103**, 933 (1995); **103**, 921 (1995).
[21] E. J. Heller, J. Chem. Phys. **75**, 2923 (1981).
[22] (a) V. S. Filinov, Nucl. Phys. B **271**, 717 (1986); (b) N. Makri and W. H. Miller, Chem. Phys. Lett. **139**, 10 (1987).
[23] J. D. Doll, D. L. Freeman, and T. L. Beck, Adv. Chem. Phys. **78**, 61 (1994).
[24] J. H. Van Vleck, Rev. Mod. Phys. **23**, 213 (1951).
[25] See, for example, R. N. Porter, L. M. Raff, and W. H. Miller, J. Chem. Phys. **63**, 2214 (1975).
[26] (a) V. A. Mandelshtam and H. S. Taylor, J. Chem. Phys. **107**, 6577 (1997); (b) D. W. Noid, B. Broocks, S. K. Gray, and S. L. Marple, J. Phys. Chem. **92**, 3386 (1988).
[27] P. M. Morse and H. Feshbach, *Methods of Theoretical Physics* (McGraw-Hill, New York, 1953), Vol. 1, p. 467.